

# **EXPERIMENTAL STUDY ON WATER WETTING AND CO<sub>2</sub> CORROSION IN OIL-WATER TWO-PHASE FLOW**

Chong Li, Xuanping Tang, Francois Ayello, Jiyong Cai and Srdjan Nestic

Institute for Corrosion and Multiphase Technology  
Ohio University  
342 W. State St., Athens, OH 45701  
U.S.A

C. Ivan T. Cruz and Jamal N. Al-Khamis

Saudi Aramco Oil Company  
Box 6891  
Dhahran, 31311  
Saudi Arabia

## **ABSTRACT**

Internal corrosion occurs only when corrosive water wets the pipe inner wall. However, water wetting is one of most important missing links of our current overall understanding of internal corrosion of oil and gas pipelines.

In this study, extensive experimental studies on water wetting in large diameter horizontal oil-water pipe flows were carried out. Four main techniques (wall conductance probes, Fe<sup>2+</sup> concentration monitoring, wall sampling and flow pattern visualization) were used to determine phase wetting on the internal wall of pipe at different superficial oil and water velocities. Four flow patterns were observed: stratified flow, stratified flow with mixed layer, semi-dispersed and dispersed flows. Three types of phase wetting regimes (water wetting, intermittent wetting and oil wetting) were determined. A comprehensive phase wetting map was obtained based on the overlapping information from these techniques.

Based on the results of corrosion monitoring, it was found that a complete absence of corrosion is guaranteed only when oil wetting occurs. At the same superficial oil velocity, the corrosion rate under water wetting is much higher than that under intermittent wetting. Phase wetting significantly affects the corrosion rate.

A comparison was carried out between the mechanistic water entrainment and separation model<sup>8-9</sup> and experimental results. A good agreement was achieved.

**Keywords:** experimental study, water entrainment, water wetting, CO<sub>2</sub> corrosion, oil-water flow

## INTRODUCTION

In the petroleum industry, mixtures of oil and water are transported over long distances in large-diameter pipelines. The presence of free water in pipelines may cause internal corrosion of the pipe walls. Corrosive gases such as carbon dioxide (CO<sub>2</sub>) and hydrogen sulfide (H<sub>2</sub>S) are also commonly present in these systems. These gases dissolve into the water phase, which may cause internal corrosion in the pipelines. Typically at low water cuts (content) and high velocities this is not an issue as all the water is entrained by the flowing oil. As the water cut increases, water “break-out” may occur, leading to segregated flow of separate layers of water and oil phases. Therefore, the possibility of corrosion is high where the water phase wets the pipe walls (typically at the bottom).

In the past, the effect of multiphase oil-water flow on CO<sub>2</sub> corrosion has been considered only in a qualitative sense. Highly turbulent flow at low water cuts was associated with negligible corrosion, whereas low flow rates or intermittent flow at higher water cuts has been associated with corrosive conditions. Hence, it is a challenge for corrosion engineers to determine more precisely the flow conditions leading to corrosion and conversely the conditions leading to entrainment of the free water layer by the flowing oil phase.

In 1975, Wicks and Fraser<sup>1</sup> published the first research paper on water entrainment. They proposed a simplified model for predicting the critical velocity of the flowing oil phase required to sweep out settled water. However, their model is suitable primarily for very low water cut situations. At high water cut, the model underestimates the critical velocity without considering the coalescence of water droplets. Since then, some efforts on this topic by a few researchers were implemented to establish empirical prediction models. However, no extensive experimental research and mechanistic modeling was involved. Wu<sup>2</sup>(1995) modified Wicks and Fraser<sup>1</sup> model without a big improvement in the performance. Smith et al.<sup>3</sup>(1987) pointed out that some oils could carry water up to 20% water cut at velocities larger than 1 m/s. From the original experiments of Wicks and Fraser<sup>1</sup>, C. de Waard and Lotz<sup>4</sup>(1993) declared a binary water-wetting prediction factor suggesting that oil-wetting will occur only for water cuts less than 30% and velocities larger than 1 m/s, when all water can be entrained in the oil phase. Adams et al.<sup>5</sup>(1993) claimed that three phase wetting (oil, intermittent and water wettings) could exist. They estimated that below 30% water cut the tubing will be oil-wet; from 30-50%, intermittent water wetting occurs, and over 50% the tubing is water wetting. Obviously, they neglected or oversimplified the effects of the properties of the oil and water phases, the flow regime and the flow geometry. Furthermore, field experience suggests that in some cases corrosion was obtained at water cuts as low as 2%, in others no corrosion was obtained for water cuts as high as 50%. C. de Waard et al.<sup>6</sup>

(2001) updated the original C. de Waard and Lotz<sup>4</sup> empirical model (1993) and proposed a new empirical model using an analysis based on the emulsion breakpoint approach. This was a major step forward from the original model, however, while agreeing reasonably well with the specific pool of field cases used for its calibration, the new model remains an empirical correlation built on limited field data with an uncertain potential for extrapolation. More importantly, this model does not consider the effect of pipe diameter, physical and chemical properties of oil phase, flow regime and system temperature on the critical velocity of the flowing oil phase required for entrainment.

As a part of Ohio University's newly released software package MULTICORP V3.0<sup>7</sup>, an advanced mechanistic model (Cai et al. <sup>8-9</sup>) of water wetting prediction in oil/water and gas/oil/water systems is included. The effects of pipe diameter, pipe inclination, oil density, oil viscosity and system temperature on the critical velocity of the flowing oil phase required for entrainment are considered in that model <sup>8-9</sup>. It should be pointed out that so far the model has not been verified in three-phase flow and does not consider the effect of type of gas, steel surface state, chemical additives and type of crude oil on water wetting because of lack of experimental and field data.

To understand the mechanism of water entrainment in the oil-water pipe flows, it is necessary to look closer into different flow regimes that occur. The main difficulties in understanding and modeling of the behavior of oil-water flows arise from the existence of the interfaces between the phases. The internal structures of two-phase flow can be best described by the flow patterns. The momentum and mass transfer mechanisms between the two phases significantly depends on the flow patterns. Also, flow patterns can indicate the phase wetting the pipe wall, position of the phases and the degree of mixing during the flow. A few studies<sup>10-25</sup> are dedicated to flow of two immiscible liquids such as water and oil. However, it should be pointed out that most of these studies focused on the macroscopic phenomena related to flow structure, such as flow regimes and flow characteristics of two immiscible liquids in the pipelines. Less attention and effort was allocated to investigating the interaction between liquids and pipe wall and the phase wetting issue, which is very important for corrosion engineers and helps them to determine the possibility of internal corrosion in the pipeline.

Typical flow patterns observed in the horizontal pipe flows are given in the FIGURE 1. Stratified flow with a complete separation of water and oil phases may exist at very low flow rates where the stabilizing gravity force due to a finite density difference is dominant. With increasing the flow rate, the interface displays a wavy character with possible entrainment of droplets at one side or both sides of the interface (semi-stratified flow). The entrainment processes for both phases increase with the flow rates. When the pure water and oil layers are still continuous at the bottom and top of the pipe respectively, and a layer of dispersed droplets exists at the interface, a three-layer structure is formed. At sufficiently high oil flow rate and low water cut, the entire water phase becomes discontinuous in a continuous oil phase resulting in a water-in-oil dispersion. Vice versa, at sufficiently high water flow rate and a high water cut, the entire oil phase becomes discontinuous in a continuous water phase resulting in an oil-in-water dispersion. There are operating conditions under which an oil-in-water dispersion will change to water-in-oil dispersion. This phenomenon is referred by lots of researchers as "phase inversion" and is associated with an abrupt change in the frictional pressure drop and a switch of the phase wetting the pipe wall from water to oil phase.

In order to validate and improve the current mechanistic water wetting model<sup>8-9</sup> with more experimental data from large diameter pipelines, comprehensive experiments were carried out to determine the phase wetting and are reported below. In this study four main overlapping techniques were used: wall conductance probes, corrosion monitoring, fluid sampling and flow pattern visualization, at different superficial oil and water velocities in large diameter horizontal oil-water pipe flows. Based

on experimental results, a phase wetting map was built. The phase wetting map can be used as a reference for calibrating water wetting models but also as a guideline for corrosion engineers and field operators which can help them assess the risk of internal corrosion in oil transportation pipelines.

## BACKGROUND OF THE WATER SEPARATION AND ENTRAINMENT MODEL

In the following sections, brief descriptions of water entrainment and separation model (Cai et al. 8-9 ) will be introduced. The model has been integrated into the University's corrosion in multiphase flow software package<sup>7</sup>.

### Water Entrainment

To extract a valid criterion for water separation and entrainment a new approach following Brauner<sup>26</sup> and Barnea<sup>28</sup> has been adopted. A criterion for forming stable water-in-oil dispersed flow is derived as the means of calculating the critical velocity for water entrainment. Two main physical properties, maximum droplet size,  $d_{max}$ , related to breakup and coalescence and critical droplet size,  $d_{crit}$ , related to settling and separation are compared to deduce this criterion. Since water is entrained by the flowing oil phase in the form of droplets, it is essential to know the maximum droplet size  $d_{max}$  that can be sustained by the flow without further breakup. In dilute water-in-oil dispersion  $d_{max}$  evolves from a balance between the turbulent kinetic energy and the droplet surface energy. For the dilute dispersion Brauner<sup>26</sup> shows that:

$$\left(\frac{d_{max}}{D}\right)_{dilute} = 1.88 \left[ \frac{\rho_o (1 - \varepsilon_w)}{\rho_m} \right]^{-0.4} We_o^{-0.6} Re_o^{0.08} \quad (1)$$

Where:

$$Re_o = \frac{\rho_o D U_c^2}{\eta_o} \quad We_o = \frac{\rho_o D U_c^2}{\sigma}$$

where  $D$  and  $d_{max}$  denote the pipe diameter and maximum droplet size, respectively, in  $m$ .  $\varepsilon_w$  presents the water cut.  $\rho$  denotes the density of liquid, in  $kg\ m^{-3}$ . The subscripts  $o$ ,  $m$  and  $dilute$  present the oil phase, the oil-water mixture and dilute oil-water dispersion, respectively.  $f$  is the friction factor.  $\eta_o$  denotes the viscosity of oil phase, in  $Pa.s$ .  $\sigma$  presents the oil surface tension, in  $Nm^{-1}$ .

It is noted that this equation can be only used in the dilute dispersions i.e. as long as it satisfies the following condition:

$$(1 - \varepsilon_w) \frac{\rho_o}{\rho_m} \cong 1 \quad (2)$$

In dense dispersions, droplet coalescence takes place. Under such conditions, the flowing oil phase disrupts the tendency of the water droplets to coalesce. Brauner<sup>26</sup> has shown that this leads to:

$$\left(\frac{d_{\max}}{D}\right)_{dense} = 2.22C_H^{0.6} \left(\frac{\rho_o U_c^2 D}{\sigma}\right)^{-0.6} \left(\frac{\varepsilon_w}{1-\varepsilon_w}\right)^{0.6} \left[\frac{\rho_m}{\rho_o(1-\varepsilon_w)} f\right]^{-0.4} \quad (3)$$

where  $U_c$  denotes the velocity of continuous phase, in  $ms^{-1}$ .  $C_H$  is a constant with the order of one,  $O(1)$ .  $D$  and  $d_{\max}$  denote the pipe diameter and the maximum droplet size, respectively, in  $m$ .  $\varepsilon_w$  presents the water cut.  $\rho$  denotes the density of liquid, in  $kg\ m^{-3}$ . The subscripts  $o$ ,  $m$  and *dilute* present the oil phase, the oil-water mixture and dilute oil-water dispersion, respectively.  $\sigma$  presents the oil surface tension, in  $Nm^{-1}$ .  $f$  is the friction factor:

$$f = 0.046 / Re_o^{0.2} \quad (4)$$

Thus, given a water-oil fluid system and operational conditions, the maximum droplet size that can be sustained is the larger of the two values obtained via (1) and (3), which can be considered as the worst case for a given oil-water system:

$$\frac{d_{\max}}{D} = Max \left\{ \left(\frac{d_{\max}}{D}\right)_{dilute}, \left(\frac{d_{\max}}{D}\right)_{dense} \right\} \quad (5)$$

Droplets larger than a critical droplet size  $d_{crit}$  separate out from the two-phase flow dispersion either due to gravity forces, predominant in horizontal flow, or due to deformation and “creaming” typical for vertical flow<sup>28</sup>. *Critical droplet diameter*,  $d_{cb}$ , above which separation of droplets due to gravity takes place can be found via a balance of gravity and turbulent forces as<sup>28</sup>:

$$\left(\frac{d_{cb}}{D}\right) = \frac{3}{8} \frac{\rho_o}{|\Delta\rho|} \frac{fU_c^2}{Dg \cos(\theta)} = \frac{3}{8} f \frac{\rho_o}{\Delta\rho} Fr_o \quad (6)$$

Where Froude number is:

$$Fr_o = \frac{U_c^2}{Dg \cos(\theta)}$$

and

$$\Delta\rho = |\rho_o - \rho_w|$$

Where  $D$  and  $d_{cb}$  denote the pipe diameter and the *critical droplet size*, respectively, in  $m$ .  $\rho$  denotes the density of liquid, in  $kg\ m^{-3}$ . The subscripts  $o$  and  $w$  present the oil phase and water phase, respectively and  $\theta$  denotes the inclination of pipe, in *degree*.

This effect is predominant at low pipe inclinations i.e. in horizontal and near-horizontal flows. Critical droplet diameter,  $d_{c\sigma}$ , above which drops are deformed and “creamed”, leading to migration of the droplets towards the pipe walls in vertical and near-vertical flows, can be calculated with the equation proposed by Brodkey<sup>29</sup>:

$$\left( \frac{d_{c\sigma}}{D} \right) = \left[ \frac{0.4\sigma}{|\rho_o - \rho_w| g D^2 \cos(\beta)} \right]^{0.5} \quad (7)$$

$$\beta = \begin{cases} |\theta| & |\theta| < 45^\circ \\ 90 - |\theta| & |\theta| > 45^\circ \end{cases}$$

Where  $D$  and  $d_{c\sigma}$  denote the pipe diameter and the *critical droplet size*, respectively, in  $m$ .  $\rho$  denotes the density of liquid, in  $kg\ m^{-3}$ . The subscripts  $o$  and  $w$  present the oil phase and water phase, respectively.  $f$  is the friction factor.  $\theta$  denotes the inclination of pipe, in *degree*.  $\sigma$  presents the oil surface tension, in  $Nm^{-1}$ .

The critical droplet diameter,  $d_{crit}$ , can then be conservatively estimated for any pipe inclination according to the suggestion made by Barnea<sup>28</sup> (1987):

$$\frac{d_{crit}}{D} = \text{Min} \left\{ \left( \frac{d_{cb}}{D} \right), \left( \frac{d_{c\sigma}}{D} \right) \right\} \quad (8)$$

At this point the final criterion for entrainment emerges. The transition from stratified flow to stable water-in-oil dispersion takes place when the oil phase turbulence is intense enough to maintain the water phase broken up into droplets no larger than  $d_{max}$  which has to be smaller than the a critical droplet size  $d_{crit}$  causing droplet separation. The transition criterion is then (Brauner<sup>26</sup>, 2001):

$$d_{max} \leq d_{crit} \quad (9)$$

Equations (5) and (8) into (9) give means to determine the critical velocity.

## Water Separation

If the water phase is not entirely entrained and flows separated from the oil phase, for corrosion calculations it is crucial to predict the water film velocity, water film thickness and the area of the internal pipe wall wetted by water at different flow regimes.

Stratified oil-water mixture structure exists in the horizontal and downward inclined pipe flows (FIGURE 2). In this study, the model is also based on a three-layer flow structure. All the interfaces are considered to be flat as proposed by Neogi et al.<sup>30</sup> and Taitel et al.<sup>31</sup>. The details of the theory are given elsewhere<sup>8</sup>. In a nutshell, the momentum and mass balances for oil, water and oil-water mixed layer are solved simultaneously to obtain the in-situ velocities for pure water layer, oil-water mixed layer and pure oil layer, as well as the thickness of pure water layer and the corresponding water wetted pipe cross-section area. This information is needed for accurate corrosion prediction.

## EXPERIMENTAL SETUP

### Experimental Layout

The experiments have been conducted at the Institute for Corrosion and Multiphase Technology at Ohio University in a 200' long, 4" ID multiphase flow loop mounted on a fully inclinable rig. The

multiphase flow rig is specially designed to investigate corrosion and multiphase flow under realistic flow conditions found in the field. FIGURE 3 shows the schematic of the fully inclinable multiphase flow rig. The same experimental setup was used for experiments by Cai et al.<sup>34</sup>

Oil is stored in a 1.2-m<sup>3</sup> stainless steel storage tank. The tank is equipped with two 1-KW heaters and stainless steel cooling coils to maintain a constant temperature. Water with 1% wt. NaCl is stored in a 1.2 m<sup>3</sup> stainless steel storage tank. Oil is pumped separately through the system using a positive displacement pump equipped with a variable speed motor. The oil flow rate is precisely controlled within a range of 0.5 to 3 m/s with a combination of the variable motor speed and a bypass system. Two separate positive displacement pumps (one for small and the other for a high flow rate) are used to pump water through the system from the water storage tank.

Oil and water are brought into contact in a T-section. The oil-water mixture flows through a 3 m-length flexible hose, which allows rig inclination to be set at any angle, and then enters the 10 cm (4 inch) I.D., 14 m long straight stainless steel pipe where the flow pattern and phase wetting develop and stabilize. The fluids then flow through a 2 m-long test section, where most measurements are carried out. The test section is made of carbon steel. A 2 m-long transparent pipe is connected downstream of the carbon steel test section, which is used to visualize the flow pattern. After that the oil-water mixture flows through a 180-degree bend, and it enters into another 14-m long stainless steel pipe and another carbon steel test section and another transparent pipe. For inclined flow the two test sections are used for distinguishing water wetting in ascending and descending flow. After the oil-water mixture leaves the downstream test section, it flows through a 20 m long 4-inch I.D PVC pipe and enters into the oil-water separator. After oil and water separate, water accumulates in the water boot and it flows through the valve at the bottom back to the water storage tank. A pure oil phase flows through the oil-outlet pipe back to the oil storage tank for further circulation.

It should be pointed out that all the surfaces in contact with the fluids, except the test sections in this multiphase flow rig, are made of corrosion-free materials (either stainless steel, epoxy or PVC).

### **Oil-Water Separator**

The oil/water separator is a crucial element in the experimental setup and enables accurate individual dosing of the liquids and prevents emulsion buildup. FIGURE 4 shows the internal structure of the oil-water separator. In order to enhance the separation efficiency, three main internal components are installed into the separator. A liquid distributor is set at the side close to the oil-water mixture inlet, which is used to distribute the oil-water mixture uniformly on the cross-section of the separator. A droplet coalescer and four sets of enhanced plate separators follow. The coalescer is built from two materials with very different surface free energy – stainless steel and plastic enabling more effective separation. The rate of coalescence is significantly increased when dispersed droplets are captured and meet at the interstices of the two dissimilar materials.

The separator is made of carbon steel and is carefully coated with corrosion resistance epoxy inside. In order to determine the separation efficiency of the oil-water separator, two sampling ports for water and oil samples are installed. The water sampling port is located at the water boot and the oil sampling one is installed on the oil line.

### **System De-Oxygenation**

Since corrosion measurements are carried out in this study, in order to minimize the effect of oxygen on corrosion process, the whole flow system is de-oxygenated using pure carbon dioxide (CO<sub>2</sub>)

before water wetting experiments are started. The whole de-oxygenation process for this system takes about two and a half hours and the oxygen concentration in the system is below 25ppb, which is allowable for CO<sub>2</sub> corrosion measurements under this environment.

## Test Section

FIGURE 5 shows the schematic of the 2-m long carbon steel test section for the current studies. During the experiments, the test section can be corroded which leads to an increase of Fe<sup>2+</sup> ion concentration in the water phase. Five rows of wall conductance probes, one set of high frequency impedance probes, wall sampling ports and ER probe holder are installed and located at the downstream portion of test section. The test section is connected with downstream and upstream pipe sections with two clamp flanges, which allow the test section to be rotated around its axis for accurate positioning of the instrumentation described below in more detail.

## Instrumentation

In this study, four main techniques were used to determine phase wetting on the internal wall of pipe at different oil and water flow rates in the large diameter oil-water horizontal flow:

- flow pattern visualization,
- wall conductance probes,
- wall sampling and
- corrosion monitoring by ER probe and iron counts (Fe<sup>2+</sup> concentration).

Visual recording were done at the transparent test section just downstream of the main carbon steel test section. Artificial coloring of the water was used to enhance the contrast between the phases. The visual technique works well with pure model oils and fails rapidly when working with crude oils.

Wall conductance probes are used to measure the water wetting along the circumference of the pipe internal wall shown in FIGURE 6(a). The probes are epoxy-coated stainless steel pins with 0.45 mm O.D. threaded through a 0.5 I.D. hole in the pipe. Five staggered rows of 18 probes (total of 90 probes) are flush-mounted on the bottom half of the pipe wall circumference shown in FIGURE 6(b). This particular arrangement with a large number of spatially distributed probes is used to minimize the errors that plagued similar efforts in the past such as the effect of a water phase “snaking” around isolated probes. Also, this redundant configuration is very useful for characterizing intermittent wetting and for eliminating experimental outliers.

A fluid sampling method is used to measure the water/oil content very close to the surface of the pipe inner wall by extracting the fluid from the bottom of the pipe. A precisely controlled needle valve and a solenoid valve used to extract the fluid are shown in FIGURE 5. The controlling instrumentation is carefully calibrated so that the proper extraction time and suction is applied to minimize erroneous readings. Slow sampling may lead to separation of the oil and water in the sampling tubing while aggressive suction draws liquid from the bulk of the flow, both distorting the picture about the oil/water ratio at the wall.

Since a CO<sub>2</sub> saturated water/oil mixture is circulated through the flow loop it is straightforward to conduct corrosion measurements in the mild steel test section. If water wetting occurs in a given test, corrosion happens and this will manifest itself as a rise in dissolved ferrous ion (Fe<sup>2+</sup>) concentration in the water phase, which can be easily detected by sampling the water and employing a standard

colorimetric technique. An ER probe mounted in the test section can also be used to monitor the corrosion rate and indirectly determine the water wetting. Both of these techniques have a considerably longer response time (typically a few hours) when compared with the other three listed above (typically a few seconds to a few minutes).

It was anticipated that by using the four very different techniques for detection of water wetting as described above, overlapping information will be obtained which would increase the confidence in the overall conclusions results and yield a stronger base for water wetting modeling.

## RESULTS AND DISCUSSION

Four series of experiments were conducted by using an LVT200 model oil and a 1 wt% NaCl brine saturated with CO<sub>2</sub> and reported below. Different flowing conditions were examined in horizontal pipe flow. Experiments at other inclinations and with crude oils are ongoing and will be reported in subsequent publications. The most important parameters in the present test matrix are shown in Table 1 below. For the LVT200 oil, the viscosity was  $\mu=2$  cP and density was  $\rho=825$  kg/m<sup>3</sup> at room temperature. The oil surface tension and oil-water interfacial tension were 0.0284 N/m and 0.0334 N/m, respectively.

### Flow Pattern Visualization

Based on video images, four types of flow patterns, stratified flow, stratified flow with mixed layer, semi-dispersed and dispersed flows, were observed during the experiments.

#### **$V_{so}=0.5$ m/s**

Stratified flow prevails at superficial oil velocity of 0.5 m/s and water cuts ranging from 4% to 20%. For water cuts less than 7% it was observed that water was predominantly in the form of “water globs” or water-in-oil droplets, 5-10 mm in diameter, which were flowing at the bottom of the pipe. In some cases smaller water droplets occasionally “floated” into the top portion of the pipe. The interaction and coalescence between water droplets is very weak at these conditions. With increasing water cut, the interaction between droplets becomes stronger and the coalescence process is enhanced. With water cut approaching 10%, a thin continuous water layer gradually forms on the bottom of the pipe. On top of the water layer, at the oil-water interface a large number of water globs could be seen. Further increase of the water cut to 13% leads to a clearer and thicker water layer on the bottom of pipe with a few water globs at the oil-water interface. The oil-water interface becomes relatively smooth and a more picture-perfect oil-water stratified flow is obtained. However, as the water cut is increased beyond 15%, a mixed layer forms at the oil-water interface (droplets of water-in-oil and oil-in-water mixed together). This layer thickens with further increasing of the water cut and a three-layered flow pattern called “stratified flow with mixed layer” is identified (Figure 7).

#### **$V_{so}=1.0$ m/s**

At superficial oil velocity of 1 m/s, two types of flow pattern were recorded: stratified flow and stratified flow with a mixed layer. A stable water layer forms at the bottom of pipe below a water cut of 14% at this oil velocity, however the layer is predominantly in the form water-in-oil droplets, much smaller than those observed at a lower oil velocity. The interaction and the coalescence between the droplets are much stronger, however, due to higher turbulence the breakup is more intense as well and very few large droplets survive. Also due to increased turbulence, more small droplets are carried

upward into the oil phase. At water cut higher than 14%, fully stratified flow with a mixed layer forms with a thickness of the mixed layer much higher than that at superficial oil velocity of 0.5 m/s.

### **$V_{so}=1.5 \text{ m/s}$**

Semi-dispersed flow occurs at superficial oil velocity of 1.5 m/s and water cuts up to 13%. No clear water layer forms at these flow conditions. Water flows as very small droplets floating in the oil phase. The distribution of water droplets on the cross-section of pipe is not uniform; more water droplets can be seen in the bottom portion of pipe.

### **$V_{so}=2.5 \text{ m/s}$**

Increasing superficial oil velocity up to 2.5 m/s leads to fully dispersed water-in-oil flow. The size of the droplets is very small and their distribution in the cross-section of pipe is apparently uniform. It appears that all the water phase is fully entrained by the flowing oil phase.

## **Wall Conductance Probes**

During all tests, the local conductivity measurements are obtained simultaneously from an array of 93 wall conductance probes. Based on the conductivity, the phase (either water or oil) that wets each flush mounted probe tip can be determined. Each experiment is repeated five times. As an example, the results of phase wetting determined by conductance probes at superficial oil velocity of 0.5 m/s and water cut of 4.3% are shown in

Figure 8. Each data point in the figure represents the value of the phase wetting indicator  $\psi$  over the five repetitions. During all tests, it is found out that stable water wetting occurs only when the water phase continuously wets the bottom of the pipe wall and there is a water layer existing at the bottom of pipe. Similarly, stable oil wetting takes place when all of the water is entrained by the flowing oil phase and water flows as droplets in the oil phase. In all other situations, intermittent wetting prevails.

### **$V_{so}=0.5 \text{ m/s}$**

It is seen from Figure 8 that intermittent wetting prevails and no stable water wetting occurs at the bottom of pipe when the superficial oil velocity is 0.5 m/s and the input water cut is 4.3%. Oil and water alternatively wet the bottom portion of pipe wall while oil wets the upper portion of pipe wall. This result is consistent with the information from flow pattern visualization. When at the same superficial oil velocity, water cut is increased to 13% (Figure 9) this leads to the occurrence of water segregation at the bottom of the pipe and water wetting occurs at the bottom. The area wetted by oil phase decreases with increasing water cut. Further increase of water cut leads to a thicker water layer flowing at the bottom of the pipe (seen in Figure 10) and more areas are continuously wetted by the water phase.

The relationship between water cut and phase wetting at superficial oil velocity of 0.5 m/s is shown in Figure 11. It is obvious that increasing the water cut leads to a transition from intermittent wetting to full water wetting. The minimum water cut leading to stable water wetting at superficial oil velocity of 0.5 m/s is about 13%.

### **$V_{so}=1.0 \text{ m/s}$**

The same procedures are applied for the determination of phase wetting at superficial oil velocity of 1 m/s and different water cuts. The relationship between water cut and phase wetting is shown in Figure 12 at superficial oil velocity of 1 m/s. It is found from Figure 12 that the minimum water cut is around 14% to form stable water wetting at superficial oil velocity of 1 m/s. Obviously, the rule of

thumb, which suggests that water entrainment occurs when water cut is 30% at oil velocity of 1 m/s, is not universal.

### **$V_{so}=1.5 \text{ m/s}$**

At superficial oil velocity of 1.5 m/s and different water cuts, the relationship between water cut and phase wetting is shown in Figure 13. It is clear that no stable water layer forms and hence no stable water wetting exists. At water cut lower than 7.5%, all of the water is entrained by the flowing oil phase. Water-in-oil dispersed flow was observed with the visual technique. The flow pattern corresponds to a stable oil wetting. Increasing water cut leads to a transition from water-in-oil dispersed flow to water-in-oil semi-dispersed flow since the turbulence is not high enough to prevent the coalescence of water droplets. More water phase exists at the bottom portion of pipe. Some water droplets occasionally contact and wet the bottom of pipe wall. This flow pattern transition corresponds to the transition from stable oil wetting to intermittent wetting.

### **$V_{so}=2.5 \text{ m/s}$**

Figure 14 shows the relationship between water cut and phase wetting when superficial oil velocity is 2.5 m/s. Stable oil wetting always exists and all the water phase is entrained by the flowing oil phase. Water-in-oil dispersed flow prevails.

## **Fluid Sampling**

### **$V_{so}=0.5 \text{ m/s}$**

In order to confirm the accuracy of results obtained from the wall conductance probes and flow pattern visualization, fluid sampling at the wall is used. Table 2 shows the results from sampling done at the same flow conditions as described above. At superficial oil velocity of 0.5 m/s and water cut up to 10%, it is seen that liquid sampling recovers about 99% water and 1% of oil. This is consistent with the occurrence of intermittent wetting determined by wall conductance probes. When the input water cut is higher than 13%, fluid sample only includes water. This denotes that a pure water layer is formed at the bottom of pipe. This information further confirms the existence of stable water wetting obtained from wall conductance probes (Figure 8 and Figure 10) and flow pattern visualization at this flow condition.

### **$V_{so}=1.0 \text{ m/s}$**

The results from wall sampling method for oil velocity of 1 m/s (shown in Table 3) are consistent with those obtained from wall conductance probes and flow pattern visualization. Compared to the results at superficial oil velocity of 0.5 m/s, it is clear that water concentration in the fluid sample decreases from 99% to 50 % with increasing superficial oil velocity from 0.5 m/s to 1.0 m/s at the same superficial water velocity of around 0.02 m/s. That means that more oil flows into the water phase since higher oil flow rate leads to higher turbulence and higher mixing between oil and water phases.

### **$V_{so}=1.5 \text{ m/s}$**

The results of fluid composition from wall sampling at superficial oil velocity of 1.5 m/s are shown in Table 4. It is found that oil and water form a suspension. It took about 2 minutes for water and oil in the sample to separate completely. Water concentration in the sample is measured after its complete separation. At a superficial oil velocity of 1.5 m/s, the water concentration in the sample increases from 1 % to 60% with increasing superficial water velocity from 0.019 m/s to 0.22 m/s. The type of suspension for the oil-water mixture close to the bottom of pipe can be determined from the water concentration in the water samples. When the water concentration in the sample is lower than 20%, the local oil-water mixture close to the bottom of pipe wall is a water-in-oil suspension, which oil phase

is a continuous phase and the water is dispersed, and apparently oil wets the bottom of pipe wall. This is consistent with the information obtained from wall conductance probes. However, when the water concentration in sample is higher than 40%, the local oil-water mixture close to the bottom of pipe could be in the transition area from water-in-oil to oil-in-water suspension since the phase inversion point for LVT200 oil occurs at water cut of 40% to 60% (Shi<sup>24</sup>). In this case, oil and water alternatively wet the bottom of pipe wall. This also confirms the results that intermittent wetting is detected by wall conductance probes.

### **$V_{so}=2.5$ m/s**

Fluid sampling results for oil velocity of 2.5 m/s are shown in and Table 5. Overall the results are qualitatively similar to those obtained at 1.5 m/s, however, it should be noted that the stability of the suspension at the superficial oil velocity of 2.5 m/s is higher. Since the water concentration in fluid samples ranged from 2% to 5%, the local oil-water mixture close to the bottom of pipe wall can be characterized as water-in-oil suspension with oil wetting the pipe wall, which confirms the results from wall conductance probes.

### **Corrosion Measurement**

In order to check and confirm the results from flow pattern visualization, wall conductance probes and wall sampling, Fe<sup>2+</sup> concentration monitoring (iron counts) was employed in this study.

Table 6 shows the results of Fe<sup>2+</sup> concentration changes in the flow loop water for three different representative phase wettings situations (oil wetting, intermittent wetting and water wetting). It is seen that the Fe<sup>2+</sup> concentration was constant under oil wetting conditions meaning that no corrosion occurs, what was expected. However, corrosion was detected by an increase in Fe<sup>2+</sup> concentration under water wetting and intermittent wetting conditions. It is indicative that the corrosion rate was retarded under intermittent conditions when compared to full water wetting. Due to an unknown area of attack it is hard to calculate the exact values for the corrosion rate.

### **Phase Wetting Map**

When all the results were cross validated by the various techniques, the data were pulled together in the form of a phase wetting map shown in Figure 15. Intermittent wetting is dominant at oil-water mixture velocity lower than 1.5 m/s and water cut less than 10%. Water wetting occurs when water cut is higher than 10% at same oil-water mixture velocity range. However, water entrainment occurs when oil-water mixture velocity is higher than 1.5 m/s and water cut lower than 10%. In this case, all water phase flows as water droplets in the oil phase.

It should be stressed that the phase wetting map shown in Figure 15 is not universal. It is valid only for the particular model oil in horizontal flow with no chemical additives and for clean steel surfaces. Results generated subsequently show that the map can change substantially as the conditions change. However, from the phase wetting map shown in Figure 15, it is clear that the commonly used rule of thumb that water entrainment occurs at oil velocity of 1 m/s and water cut of 30% is invalid.

### **Comparison with Water Entrainment and Separation Model**

While there are no universal flow maps and rules of thumb, there should be a universal model which reflects the complex behavior described above. Figure 16 shows the comparison between the experimental results of phase wetting and the predictions by the model described above (Cai et al. <sup>8-9</sup>). The solid line in the figure represents the prediction by the model for water entrainment at different

superficial oil and water velocities. It is clear that the model<sup>8-9</sup> is in very good agreement with experimental results for the predictions of water entrainment.

It should be pointed out that only two types of phase wettings (water wetting and oil wetting, which correspond to water separation and water entrainment, respectively) can be determined by the present model<sup>8-9</sup>. This model does not further distinguish the boundary between stable water wetting and intermittent wetting as in both cases corrosion occurs.

## CONCLUSIONS

Four main techniques (flow pattern visualization, wall conductance probes, wall sampling and Fe<sup>2+</sup> concentration monitoring) are used to detect phase wetting at different superficial oil and water velocities in large diameter horizontal oil-water pipe flows. According to those experimental results, the following main points can be concluded:

- An extensive phase wetting map was built based on the overlapping information obtained from these techniques.
- Four flow patterns were observed: stratified flow, stratified flow with mixed layer, semi-dispersed and dispersed flows.
- Three types of phase wettings (water wetting, intermittent wetting and oil wetting) were determined.
- Based on the results of Fe<sup>2+</sup> concentration monitoring, it was found that a complete absence of corrosion only occurs when water entrainment (oil wetting) exists. Intermittent wetting and water wetting could lead to a potential corrosion problem.
- The water entrainment and separation model<sup>8-9</sup> agrees with experimental results very well.

## ACKNOWLEDGEMENT

Financial support from Saudi Aramco Co. for Institute for Corrosion and Multiphase Technology of Ohio University is gratefully acknowledged.

## REFERENCES

- 1 Wicks, M., and Fraser, J.P., "Entrainment Of Water By Flowing Oil", Materials Performance, May 1975, pp. 9~12.
- 2 Wu, Y., "Entrainment Method Enhanced to Account fro Oil's Water Content", Oil & Gas Technology, Aug. 28, 1995, pp. 83~86.

- 3 L.M.Smith, M.J.J. Simon Thomas and C. de Waard, "Controlling Factors in the Rate of CO<sub>2</sub> Corrosion", UK. Corr.'87 Brighton, 26-28 Oct., 1987
- 4 C. de Waard and U. Lotz, "Prediction of CO<sub>2</sub> Corrosion of Carbon Steel", Corrosion/93, paper no. 69, (Houston, TX: NACE International, 1993)
- 5 C. D. Adams, J. D. Garber, F. H. Walters, C. Singh, "Verification of Computer Modeled Tubing Life Predictions by Field Data", Corrosion/93, paper no. 82, (Houston, TX: NACE International, 1993)
- 6 C.de Waard, L.Smith and B.D. Craig, "The Influent of Crude Oil on Well Tubing Corrosion Rates", EUROCORR 2001.
- 7 S. Nestic, Jiyong Cai, Shihuai Wang, Ying Xiao and Dong Liu, Ohio University Multiphase Flow and Corrosion Prediction Software Package MULTICORP V3.0, Ohio University(2004).
- 8 Jiyong Cai, Srdjan Nestic and Cornelis de Waard, "Modeling of Water Wetting in Oil-Water Pipe Flow", NACE 2004, Paper No.04663, pp. 1-19, 2004.
- 9 Srdjan Nestic, Jiyong Cai and Kun-Lin John Lee, "A Multiphase Flow and Internal Corrosion Prediction Model for Mild Steel Pipelines", NACE 2005, Paper No.05556.
- 10 Russell, T. W. F., Hodgson, G.W., and Govier, G. W., "Horizontal Pipelines Flow of Mixtures of Oil and Water", Can. J. of ChE, 37, 9-17, 1959
- 11 Charles, M.E., Govier, G.W. and Hodgson, G.W., "The Horizontal Pipelines Flow of Equal Density Oil-water Mixture", Can. J. Chem. Eng., 39, 27-36, 1961
- 12 Ward, J.P. and Knudsen, J.G, "Turbulent Flow of Unstable Liquid-Liquid Dispersions: Drop Size and Velocity Distributions", AIChE. J., 13, No 2, 356-367, 1967
- 13 Oglesby, K. D., "An Experimental Study on the Effects of Oil Viscosity, Mixture Velocity and Water Fraction on Horizontal Oil-Water flow", M.S. Thesis, University of Tulsa, 1979
- 14 Mukherjee, H., Brill, J.P., and Beggs, H. D., "Experimental Study of Oil-Water Flow in Inclined Pipes", J. of Energy Resources Technology, 56-66, March, 1981
- 15 Arirachakaran, S., K. D., Oglesby, M. S., Malinovsky, M.S., Shoham, O., and J.P. Brill, "An Analysis of Oil-Water Flow Phenomena in Horizontal Pipes", SPE paper 18836, 155-167, 1989
- 16 Pal, R., "Pipeline Flow of Unstable and Surfactant-Stabilized Emulsions", AIChE J., 39, No.11, 1754-1764, 1993
- 17 Pal, R., "Effect of Droplet Size on the Rheology of Emulsions", AIChE J., 42, No.11, 3181-3190, 1996
- 18 Kurban, A. P. A., Angeli, P. A., Mendes-tatsis, M. A., and Hewitt, G. F., "Stratified and Dispersed Oil-Water Flows in Horizontal Pipes", Multiphase 95, 277-291, 1995
- 19 Trallero, J. L, Sarica, C and J. P. Brill, "A Study of Oil-Water Flow Patterns in Horizontal Pipes", SPE, Paper No. 36609, 363-375, 1996
- 20 Flores, J. G., Sarica, C., Chen, T. X., and Brill, J. P., "Investigation of Holdup and Pressure Drop Behavior for Oil-Water Flow in Vertical and Deviated Wells", ETCE-98, Paper No. 10797, 1997
- 21 Nadler, M. and Mewes, D, "Flow Induced Emulsification in the Flow of Two Immiscible Liquids in Horizontal Pipes", Int. J. Multiphase Flow, 23, 56-68, 1997
- 22 Angeli, P., and Hewitt, G. F, "Drop Size Distributions in Horizontal Oil-Water Dispersed Flows", Chem. Eng. Sci. 55, 3133-3143, 2000
- 23 Corlett, A.E., and Hall, A.R.W., "Viscosity of Oil and Water Mixtures", Multiphase 99, 595-603, 1999
- 24 H.Shi, "A Study of Oil-Water Flows in Large Diameter Horizontal Pipelines", Ph.D Dissertation, Ohio University, 2001
- 25 Brauner, N., Moalem Maron, "Flow Pattern Transitions in Two-phase Liquid-liquid Horizontal Tubes", Int. J. of Multiphase Flow, Vol.18, pp. 123~140(1992a).
- 26 Brauner, N., "The Prediction of Dispersed Flows Boundaries in Liquid-Liquid and Gas-liquid Systems", Int. J. of Multiphase Flow, Vol.27, pp. 885~910(2001)

- 27 Hinze, J., "Fundamentals of the Hydrodynamic Mechanism of Splitting in Dispersion Process", AICHE, Vol. 1(1955), No. 3, pp. 289~295
- 28 Barnea, D., "A Unified Model for Predicting Flow Pattern Transitions for the Whole Range of Pipe Inclinations", Int. J. of Multiphase Flow, Vol.11, pp. 1~12(1987)
- 29 Brodkey, R.S., "The Phenomena of Fluid Motions", Addison-Wesley, Reading, M.A., 1969
- 30 Neogi, S., Lee, A.H. and Jepson, W.P., "A Model for Multiphase (Gas-Water-Oil) Stratified Flow in Horizontal Pipelines", SPE 28799, pp.553-561,1994
- 31 Taitel, Y., Barnea, D. and Brill, J.P., "Stratified Three-phase Flow in Pipes", Int. J. Multiphase Flow, Vol. 21, No.1, pp. 53-60,1995
- 32 Taitel, Y. and Dukler, A.E., "A Model for Predicting Flow Regime Transitions in Horizontal and Near Horizontal Gas Liquid Flow", AICHE J., Vol.22, No.1, pp.47, 1976
- 33 N. Brauner and Maron, D.M., "Two-phase Liquid-liquid Stratified Flow", Physicochemical Hydrodynamics, Vol. 11, No.4, pp.487-506, 1989.
- 34 Jiyong Cai, Srdjan Nesic, Chong Li, Xuanping Tang, Francois Ayello, C.Ivan T. Cruz and Jamal N. Khamis, "Experimental Studies of Water Wetting in Large Diameter Horizontal Oil-Water Pipe Flows", SPE 2005, Paper No. 95512-PP.

Table 1 Main test parameters

Oil phase	LVT200 oil
Water phase	1% NaCl solution
Superficial water velocity, $V_{sw}$	0 ~ 0.22 m/s
Superficial oil velocity, $V_{so}$	0.5 ~ 2.5 m/s
Water cut, $\epsilon$	0 ~ 20%
Pipe inclination	Horizontal
Pipe diameter	4"
System temperature	25 °C
System pressure	0.13 MPa

Table 2 Water concentration in the fluid samples at superficial oil velocity of 0.5 m/s and different superficial water velocities

$V_{so}$ (m/s)	$V_{sw}$ (m/s)	Water concentration in the fluid sample (%)
0.5	0.019	99
0.5	0.022	99
0.5	0.056	99
0.5	0.074	100
0.5	0.093	100
0.5	0.11	100

Table 3 Water concentration in the fluid samples at superficial oil velocity of 1.0 m/s and different superficial water velocities

$V_{so}$ (m/s)	$V_{sw}$ (m/s)	Water concentration in the fluid sample (%)
1	0.019	50
1	0.037	75
1	0.056	90
1	0.074	95
1	0.15	99
1	0.17	100
1	0.19	100
1	0.20	100

Table 4 Water concentration in the fluid samples at superficial oil velocity of 1.5 m/s and different superficial water velocities

$V_{so}$ (m/s)	$V_{sw}$ (m/s)	Water concentration in the fluid sample (%)	Comments
1.5	0.019	1	Unstable emulsion
1.5	0.074	10	Unstable emulsion
1.5	0.11	20	Unstable emulsion
1.5	0.15	40	Unstable emulsion
1.5	0.19	60	Unstable emulsion
1.5	0.22	60	Unstable emulsion

Table 5 Water concentration in the fluid samples at superficial oil velocity of 2.5 m/s and different superficial water velocities

$V_{so}$ (m/s)	$V_{sw}$ (m/s)	Water concentration in the fluid sample (%)	Comments
2.5	0.019	5	Emulsion
2.5	0.056	5	Emulsion
2.5	0.093	4	Emulsion
2.5	0.10	2	Emulsion
2.5	0.17	2	Emulsion
2.5	0.20	2	Emulsion

Table 6  $Fe^{2+}$  concentration change under different phase wettings in LVT200 oil-water horizontal flow

Oil-water mixture velocity (m/s)	Water cut (%)	Testing time (Min.)	$Fe^{2+}$ change (ppm)	Phase wetting	pH
0.6	16	30	1.32	Water wetting	4.71
0.8	14	30	0.57	Intermittent wetting	4.86
1.6	7	30	0	Oil wetting	4.82

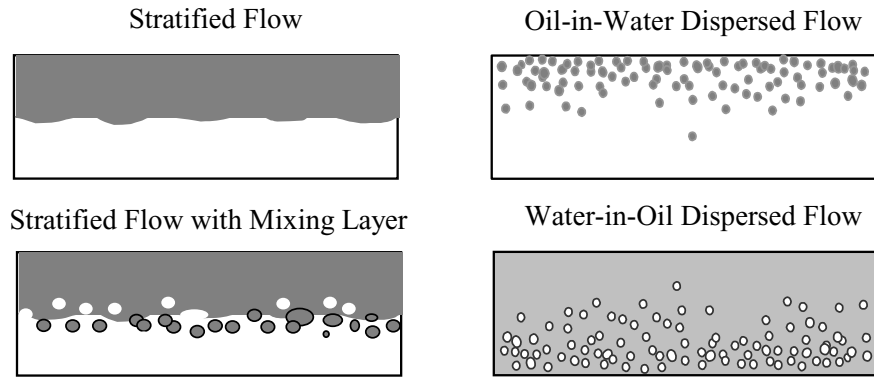


FIGURE 1. Flow patterns in oil-water horizontal flows

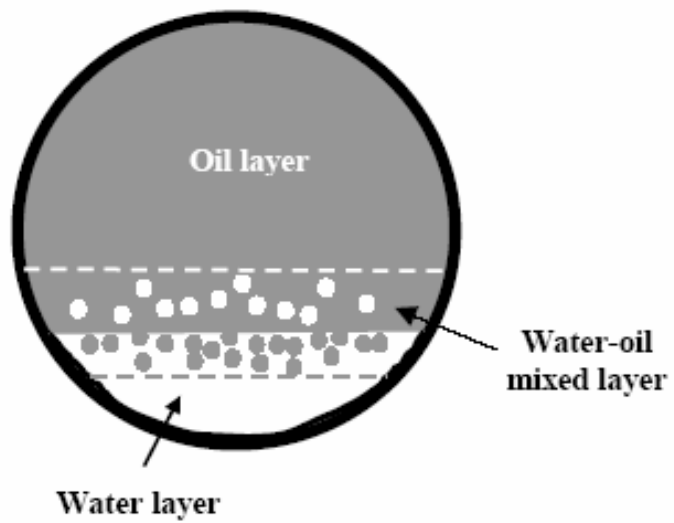


FIGURE 2. Cross-section for a three-layer structure with a planar interface

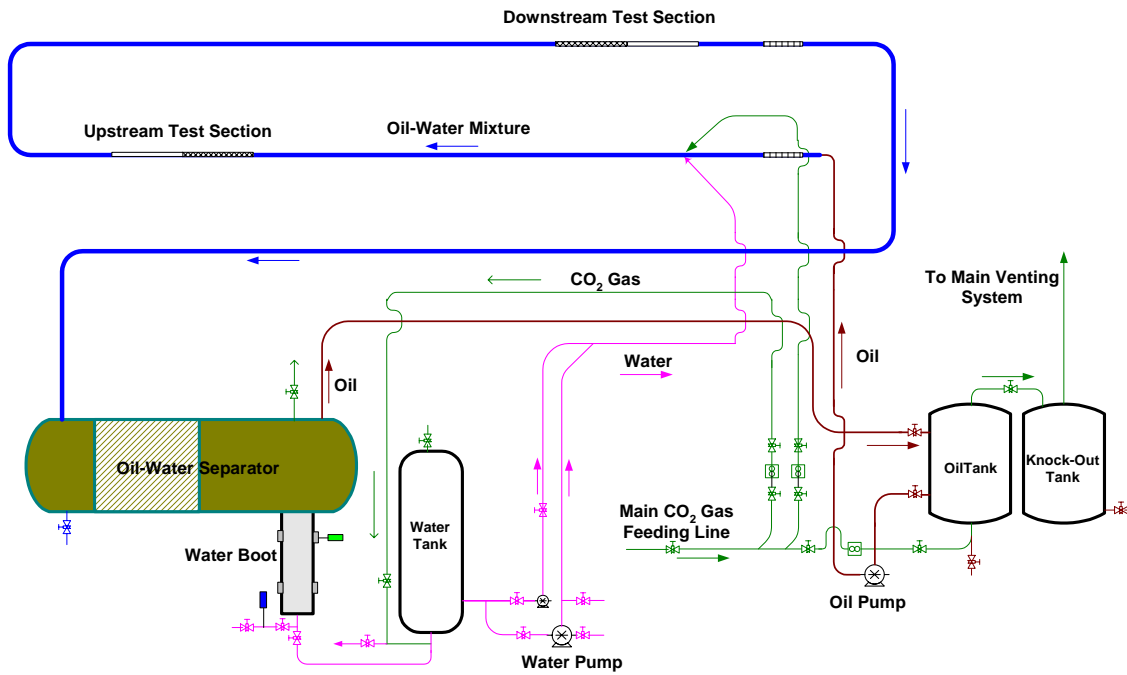


FIGURE 3. Schematic of 4-inch I.D. fully inclinable multiphase flow loop

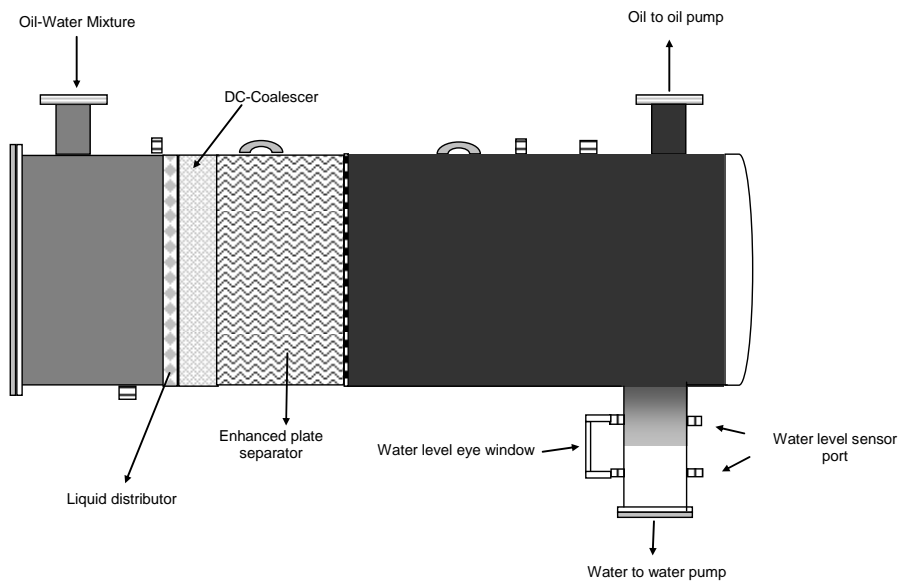


FIGURE 4. Schematic of internal components in oil-water separator

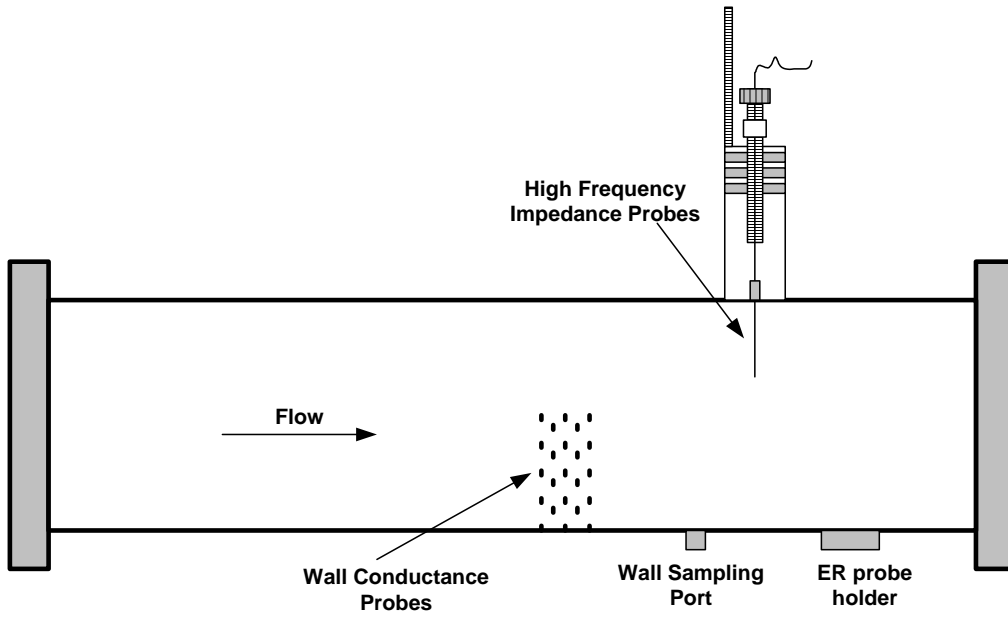
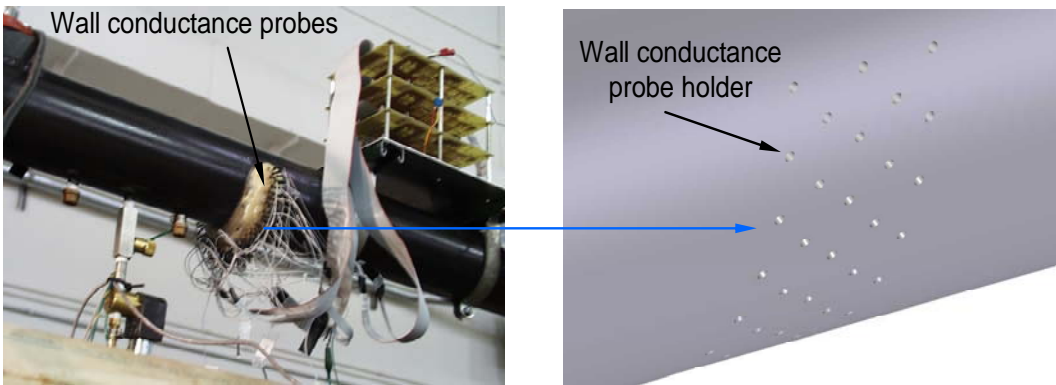


FIGURE 5. Schematic of test section



(a)

(b)

FIGURE 6. Wall conductivity probes

(a): wall conductivity probes on the test section

(b): 5 rows of staggered configuration of probe holders



Figure 7 Three-layer flow structure at superficial oil velocity of 0.5 m/s and water cut of 18% in horizontal oil-water flow (water phase is dyed with red color)

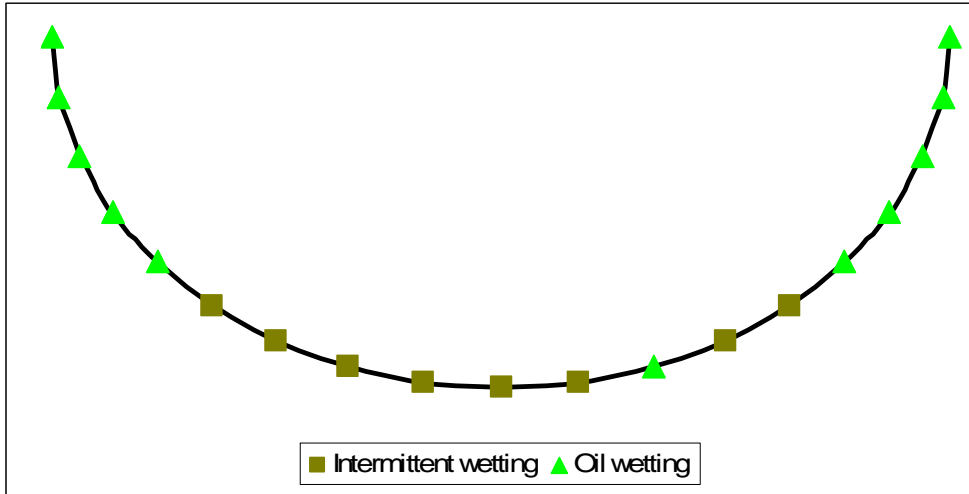


Figure 8 Results of one row of wall conductance probes on the bottom half of pipe circumference at superficial oil velocity 0.5 m/s and superficial water velocity 0.022 m/s (water cut of 4.3%)

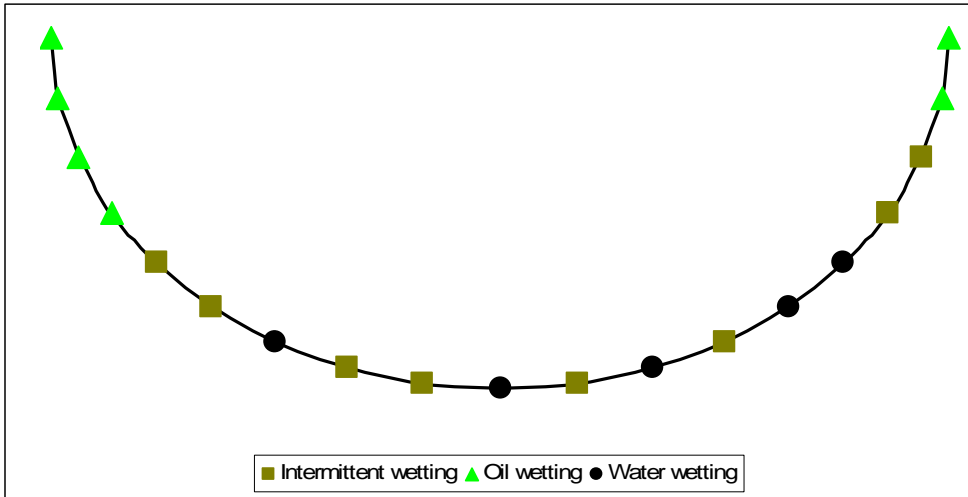


Figure 9 Results of one row of wall conductance probes on the bottom half of pipe circumference at superficial oil velocity 0.5 m/s and superficial water velocity 0.074 m/s (water cut of 13%)

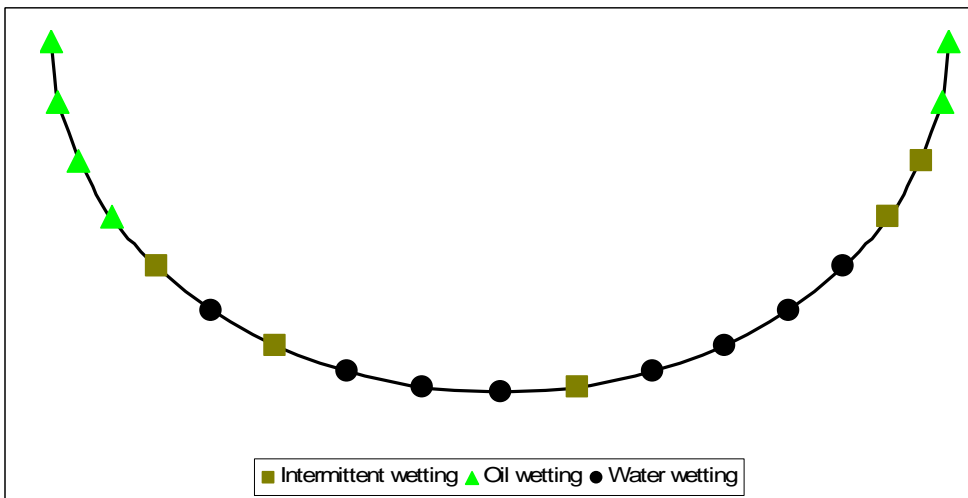


Figure 10 Results of one row of wall conductance probes on the bottom half of pipe circumference at superficial oil velocity 0.5 m/s and superficial water velocity 0.11 m/s (water cut of 18%)

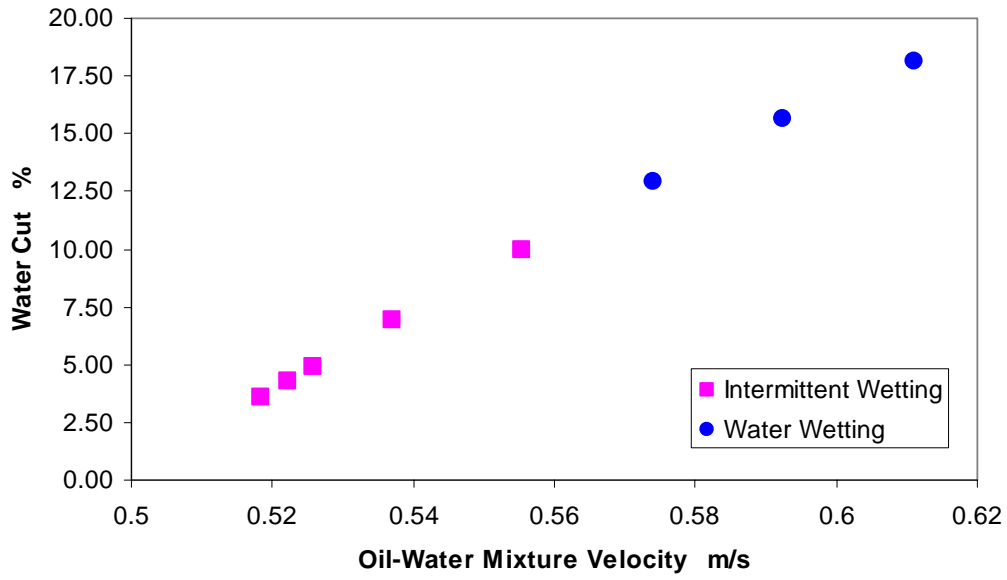


Figure 11 Relationship between water cut and phase wetting at superficial oil velocity of 0.5 m/s

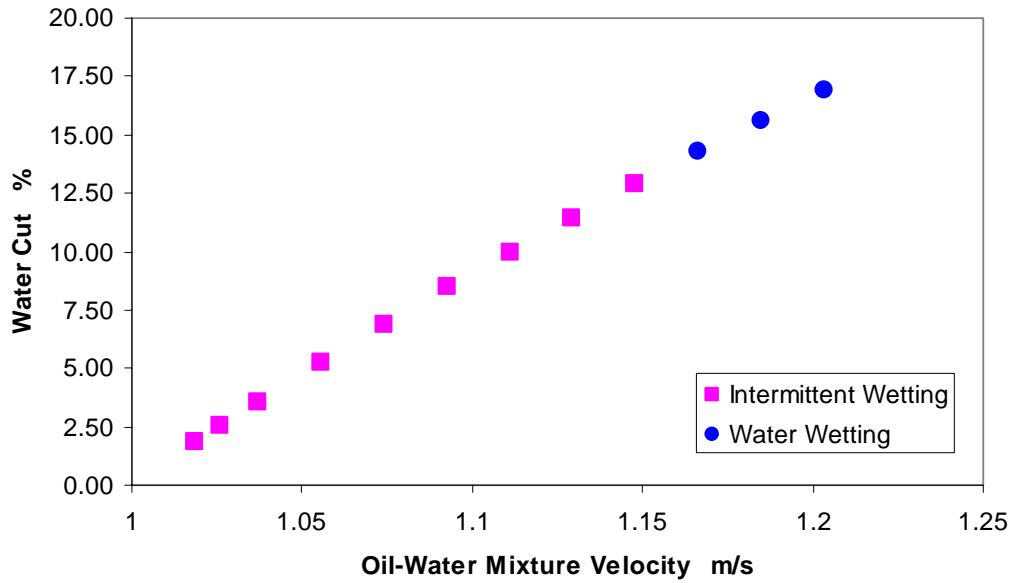


Figure 12 Relationship between water cut and phase wetting at superficial oil velocity of 1.0 m/s

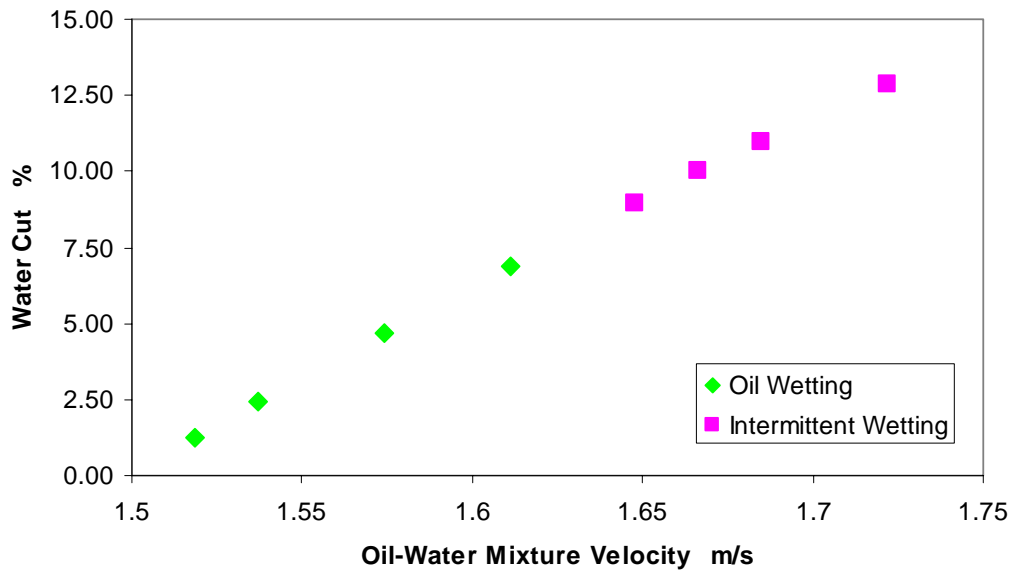


Figure 13 Relationship between water cut and phase wetting at superficial oil velocity of 1.5 m/s

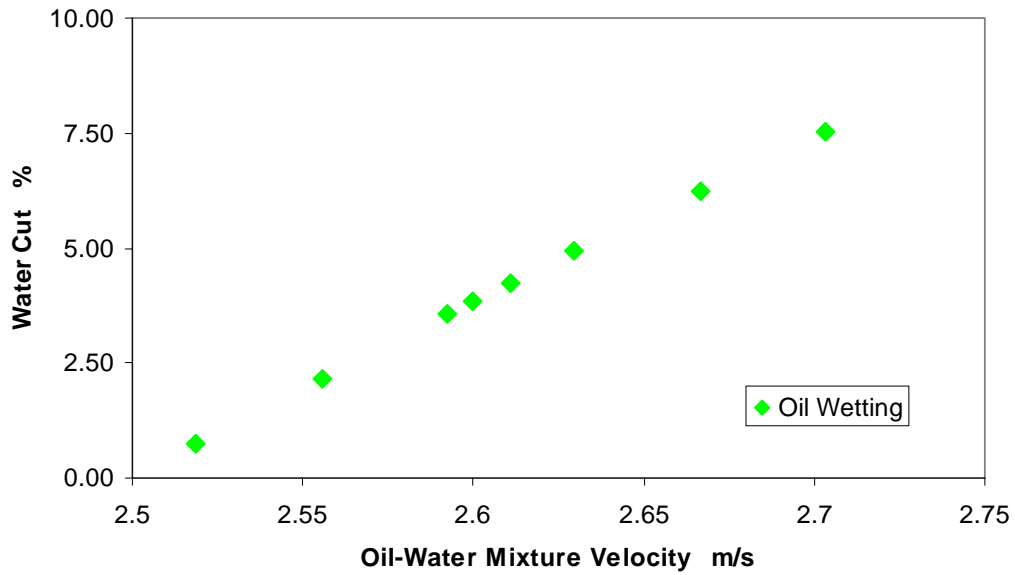


Figure 14 Relationship between water cut and phase wetting at superficial oil velocity of 2.5 m/s

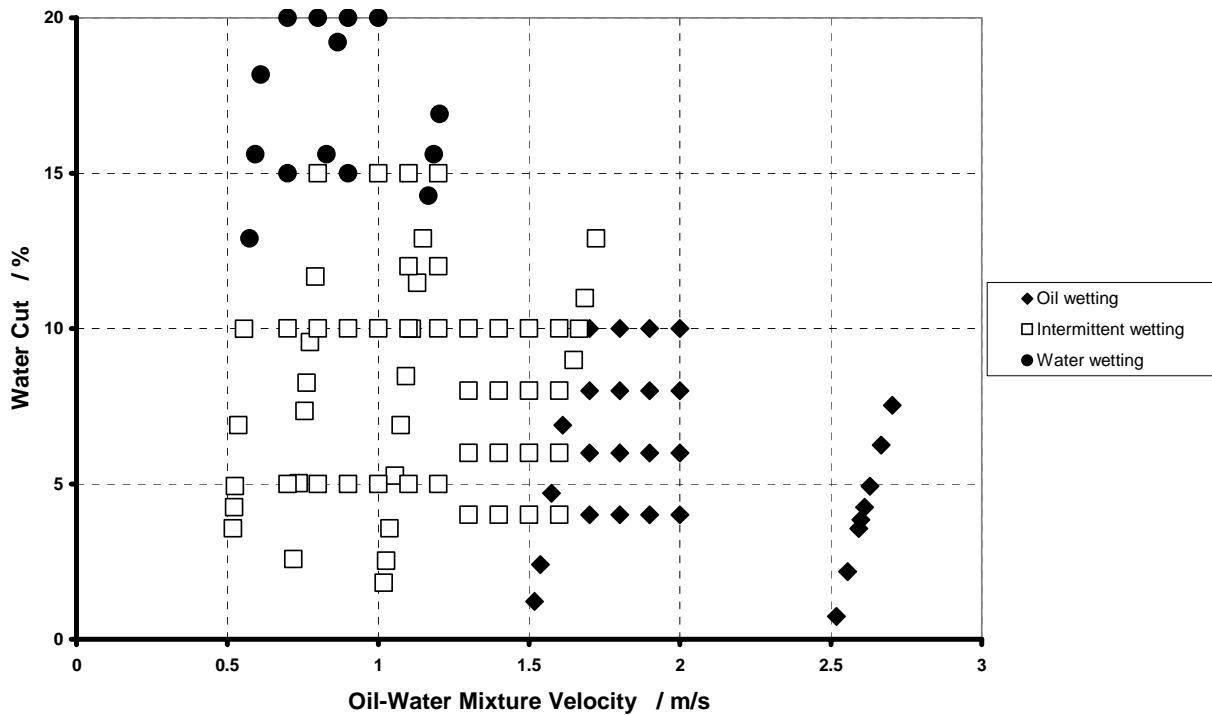


Figure 15 Phase wetting map at different oil-water mixture velocities and water cuts in the horizontal oil-water two-phase flow

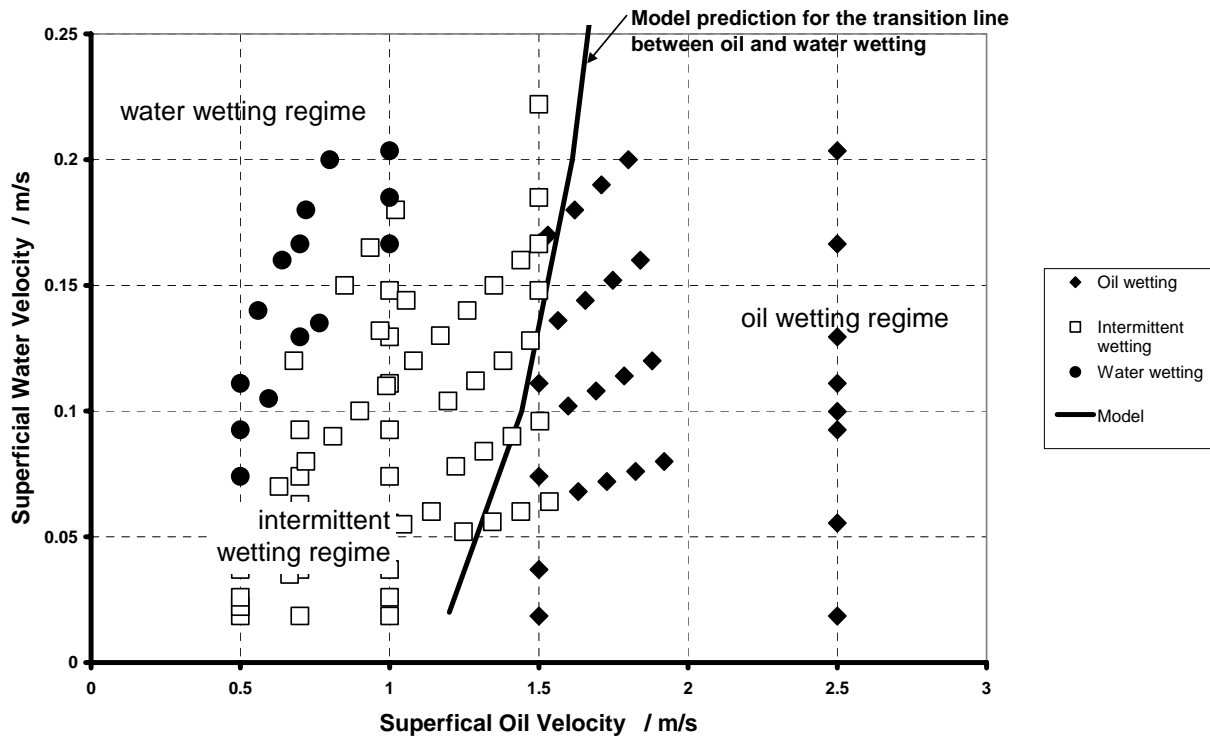


Figure 16 Phase wetting map at different superficial oil and water velocities in the horizontal oil-water two-phase flow